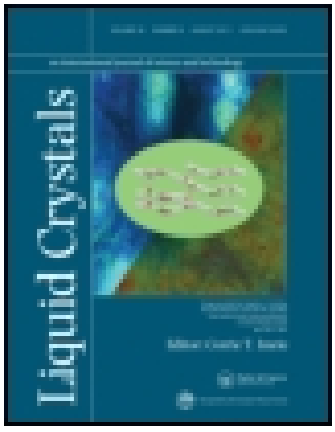

Liquid Crystals
Publication details, including instructions for authors and subscription information:
http://www.tandfonline.com/loi/tlct20

Role of the elastic constants of a liquid crystal with positive dielectric anisotropy in the electro-optic characteristics of fringe-field switching mode

Heui-Seok Jin[a], Dae Hyung Kim[a], Jin Hyun Kim[a], Han Sol Choi[a], Joong Hee Lee[a], Gi-Dong Lee[b] & Seung Hee Lee[a]

[a] Department of BIN Fusion Technology, Applied Materials Institute for BIN Convergence and Department of Polymer-Nano Science and Technology, Chonbuk National University, Jeonju, South Korea

[b] Department of Electronics Engineering, Dong-A University, Busan, Korea

Published online: 18 Jun 2015.

To cite this article: Heui-Seok Jin, Dae Hyung Kim, Jin Hyun Kim, Han Sol Choi, Joong Hee Lee, Gi-Dong Lee & Seung Hee Lee (2015): Role of the elastic constants of a liquid crystal with positive dielectric anisotropy in the electro-optic characteristics of fringe-field switching mode, Liquid Crystals, DOI: 10.1080/02678292.2015.1033772

To link to this article: http://dx.doi.org/10.1080/02678292.2015.1033772

Liquid Crystals, 2015
http://dx.doi.org/10.1080/02678292.2015.1033772

Role of the elastic constants of a liquid crystal with positive dielectric anisotropy in the electro-optic characteristics of fringe-field switching mode

Heui-Seok Jin[a], Dae Hyung Kim[a], Jin Hyun Kim[a], Han Sol Choi[a], Joong Hee Lee[a], Gi-Dong Lee[b]* and Seung Hee Lee[a]*

[a]*Department of BIN Fusion Technology, Applied Materials Institute for BIN Convergence and Department of Polymer-Nano Science and Technology, Chonbuk National University, Jeonju, South Korea;* [b]*Department of Electronics Engineering, Dong-A University, Busan, Korea*

(*Received 10 February 2015; accepted 22 March 2015*)

We investigated how the electro-optic characteristics of the fringe-field switching (FFS) liquid crystal (LC) mode are affected by elastic constants of LCs. Unlike conventional liquid crystal (LC) devices, in which mainly the dielectric torque determines reorientation of LC, the field-induced LC reorientation in the fringe-field switching (FFS) mode is controlled first by dielectric torque and then by pure elastic torque between LCs so that the transmittance oscillates along the electrode positions. We find that elastic constants of the LC play an important role on the field-induced dynamics of the LC molecules such that the higher the splay constant is, the higher the light efficiency becomes, which is a unique characteristic of the FFS mode. The results present an important design of physical properties of LC to enhance better transmittance in the FFS mode.

Keywords: liquid crystal; fringe-field switching; transmittance; elastic constant

1. Introduction

Recently, fringe-field switching (FFS) liquid crystal (LC) mode is being used mainly in liquid crystal displays (LCDs) with a high resolution, a high image quality, low power consumption and touch screen, irrespective of the size of the LCDs.[1–7] In the FFS LCDs, the electro-optics strongly depends on the sign of the dielectric anisotropy of an LC such that an LC with positive dielectric anisotropy (+LC) has advantages in lower operating voltage and faster response time than those with an LC with negative dielectric anisotropy (–LC).[8] However, the FFS LCDs with –LC shows higher transmittance and better field-induced dynamic stability than those with +LC.[9,10] The first commercialised FFS LCDs utilised –LC for position- and pressure-sensitive displays [7] in the late 1990s but since then only +LC has been applied to all high-resolution displays for portable mobiles, personal computers and televisions up to recent times because the FFS LCDs with +LC still give much better performance than other LC modes in terms of transmittance and operating voltage. In the recent few years, the resolution of mobile LCDs has increased from 326 ppi to over 500 ppi to exhibit a better image quality and then the transmittance of FFS LCDs with +LC decreased, resulting in high power consumption overall. Then, –LC in the FFS LCDs becomes an alternative for compensating the loss of the transmittance in such a high-resolution display and thus it starts to be commercialised again, although the response time and operating voltage are not satisfactory.

Electro-optic studies on the FFS mode with +LC have already been performed extensively and it was known that the transmittance of the FFS LCDs depends on many cell parameters such as electrode structure,[7,11–13] rubbing direction,[14] retardation value of the LC layer,[15,16] cell gap,[17,18] and sign and magnitude of dielectric anisotropy ($\Delta\varepsilon$).[19–22]

To improve the performance of the FFS mode and make it more efficient, one needs to know the dependence of switching behaviour on the intrinsic physical properties of the LC material. To our information, how three elastic constants, splay (K_{11}), twist (K_{22}) and bend (K_{33}), of a +LC can improve the transmittance of the FFS mode is not reported yet. In this article, we investigate the electro-optics of the FFS mode depending on the elastic constants of a +LC, especially the splay elastic constant K_{11} with experimental and simulation results.

2. Key switching principle of the FFS mode

In the FFS mode, the LCs are homogeneously aligned in an initial state with its optic axis coincident with one of the crossed polariser axes so that the cell appears to be black in the absence of an electric field. With bias voltage above Frederick's transition,

*Corresponding authors. Email: gdlee@dau.ac.kr; lsh1@chonbuk.ac.kr

the transmittance starts to generate, roughly following the equation below:

$$T/T_0 \sim \sin^2(2\phi_{\text{eff}}(V))\sin^2(\pi d\Delta n_{\text{eff}}(V)/\lambda) \quad (1)$$

where ϕ_{eff} is the voltage-dependent effective angle between one of the transmission axes of the crossed polariser and the LC director, d is cell gap, Δn_{eff} is voltage-dependent effective birefringence of LC medium and λ is the wavelength of an incident light.

In the in-plane switching (IPS) mode, the gap between signal and common electrodes is larger than cell gap and electrode width so that a pure in-plane field rotates the LC horizontally.[23] However, the FFS mode has a different electrode structure such that the gap between signal and common electrodes is smaller than cell gap and electrode width so that a fringe-electric field having both horizontal (E_y) and vertical (E_z) electric fields is generated, as shown in Figure 1 As expected from the field distribution, just above electrode surface exists a strong E_y at the edge of signal and common electrodes (position A) so that the LC just above the electrode rotates most, overcoming a strong surface-anchoring bound by alignment layer. Interestingly, there are no E_ys at the centre of the signal and common electrodes (position C), indicating that the LC cannot rotate at all by dielectric torque between E_y and $\Delta\varepsilon$ of an LC. On the other hand, a fringe electric field exists at the position between the centre and the edge of the signal (and common) electrodes (position B and D) so that a +LC will try to align parallel to the fringe electric field, generating a tilt angle with respect to the surface. The degree of that tilt angle determines the degree of twisted angle at the central position of the signal and common electrodes because the LC in that position is rotated by purely elastic torque between the LCs at positions B and D and the LC at position C. Therefore, the higher the LC is twisted at positions A and B, more twisted is the LC at position C by elastic torque and the transmittance will be maximised if the ϕ_{eff} of LC at position C reaches 45°.

Assuming that all cell parameters are the same, the FFS cell with –LC shows a higher transmittance than that with +LC, as shown in simulation results of Figure 2. The key difference between two types of LCs mainly comes from the LC orientation at positions B and D, such that the +LC shows a higher tilt angle than that with –LC because the –LC reorients

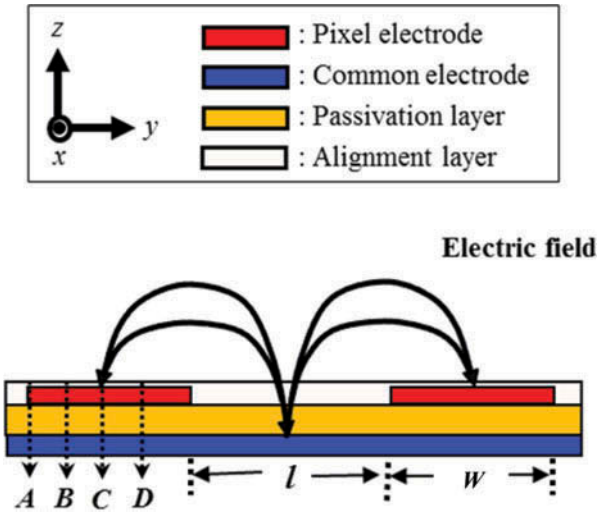

Figure 1. (colour online) Schematic electrode structure of the FFS mode with electric field lines.

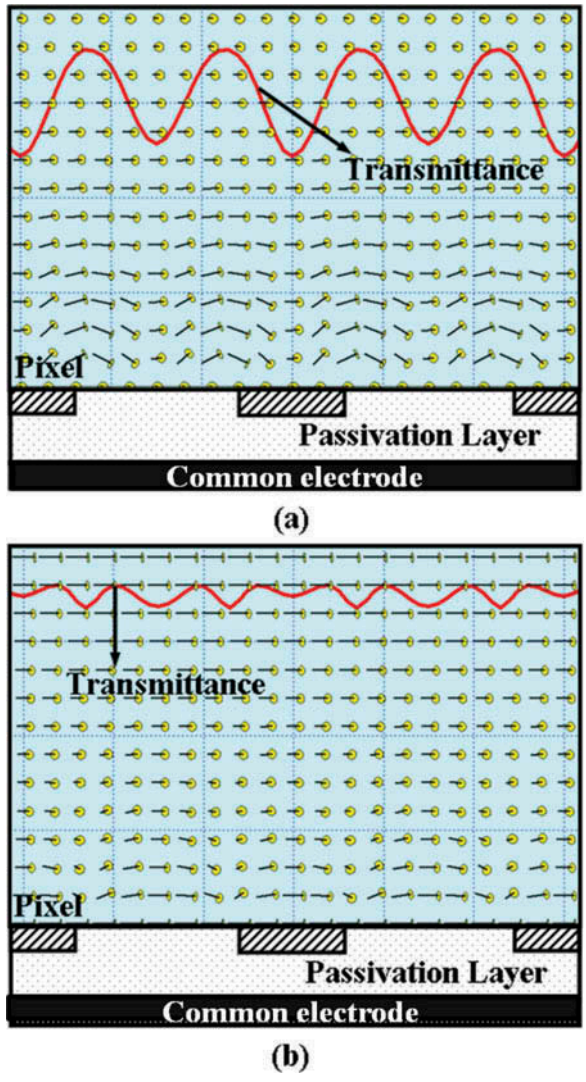

Figure 2. (colour online) Transmittance and LC orientation dependent on electrode position in the FFS mode with: (a) an LC with positive dielectric anisotropy LC and (b) an LC with negative dielectric anisotropy.

perpendicular to the fringe electric field. Consequently, the twisted angle above the centres of the pixel and common electrodes is less in the +LC than in the –LC, giving rise to lower transmittance in the +LC than in the –LC in those positions.[18] As a result, the transmittance is more strongly dependent on electrode positions in the +LC than in the –LC. Therefore, if one can suppress tilt angle at positions B and D, higher elastic torques on LC at position C will be given, generating higher rotation angle and consequently higher transmittance.

3. Results and discussion

For the purpose of electro-optic characteristic calculations, we used commercially available software, 'LCD Master' (Shintech, Japan), where the motion of the LC director is calculated based on the Ericksen–Leslie theory and 2 × 2 Jones matrix [24] is applied to achieve the optical transmittance calculation. The strong anchoring at both substrates is assumed such that the LCs will not rotate at the interface between alignment and LC layers. The detailed electrode structure and cell conditions considering a normal FFS mode is summarised in Table 1.

3.1. *Electro-optic effects depending on splay elastic constant (K_{11})*

In order to observe the K_{11} effects on the electro-optics of the FFS mode, it is varied from 8.7 to 20.7 pN while keeping the rest of the parameters unchanged with K_{22} = 5.2 pN and K_{33} = 13.3 pN. Figure 3(a) shows voltage-dependent transmittance (V–T) curves depending on K_{11}. When K_{11} is 8.7 pN, the operating voltage (V_{op}) is 4.4 V and it remains the same even if K_{11} is increased to K_{11} = 20.7 pN. Interestingly, the transmittance with a higher K_{11} shows a slightly higher value; for example, when the K_{11} is increased from 8.7 to 20.7 pN, the transmittance increases by about 5.5%, from 0.78 to 0.82, as shown in Figure 3(b). The transmittance difference mainly comes from electrode position around C, as indicated in Figure 3(c), proving that the tilt angle of LC molecules at positions B and D can be suppressed when an LC with high K_{11} is used and thus the LC at position C can be twisted more, resulting in a higher transmittance in the cell with K_{11} = 20.7 pN than that of the cell with K_{11} = 8.7 pN. In order to confirm suppression of a tilt deformation, an LC molecular orientation is calculated as shown in Figure 3(d). As clearly indicated, the maximum tilt angles at z/d = 0.025 at position A and about z/d = 0.1 at position B reduce from −36° to −29° and from −46° to −31°, respectively, when K_{11} increases from 8.7 to 20.7 pN. Here the minus tilt angle indicates that the tilt angle is formed in an opposite direction to that of an initial one. Consequently, lower tilt angles at positions A, B and D will result in higher twisted angles at each electrode position. Figure 3(e) represents twisted angles at four electrode positions. As expected, the twisted angles should increase, especially at electrode position C, and the maximum twisted angle increases from 32.6° at z/d = 0.43 to 35.4° at z/d = 0.28, which is an origin of improved transmittance with the use of LCs with higher K_{11}.

Table 1. Simulation conditions of the FFS mode.

Simulator		LCD master (Shintech, Japan)
Electrode width (μm)		3.0
Electrode distance (μm)		4.5
Cell gap (μm)		4
Pre-tilt (°)		2
Rubbing angle (°)		80
Passivation layer thickness (μm)		0.29
Rotational viscosity (mPa s)		80
LC	K_{11} (pN)	8.7–20.7
	K_{22} (pN)	3.2–8.2
	K_{33} (pN)	11.3–23.3
	Δn	0.10
	$\Delta\varepsilon$	8.2

Next, response times depending on elastic constants have been investigated. In nematic LC devices, the rise (τ_{on}) and decay (τ_{off}) times are given by [25]

$$\tau_{on} = \frac{\gamma d^2}{\pi^2 K_{eff}\{(V^2 - V_{th}{}^2) - 1\}} \quad (2)$$

$$\tau_{off} = \frac{\gamma d^2}{\pi^2 K_{eff}} \quad (3)$$

where γ is a rotational viscosity of an LC, K_{eff} is effective elastic constant of an LC and V_{th} is a threshold voltage of an LC device. In conventional IPS and vertical alignment devices,[26] LC mainly experiences twist and bend deformation with applied voltage so that K_{eff} is replaced by K_{22} and K_{33}, respectively.

Figure 3(f) shows calculated response times as a function of the amplitude of K_{11}s. Here, the response times for transmittance change of both 80% and 90% are considered. The results are very interesting such that τ_{on} becomes shorter with increasing K_{11} while τ_{off} remains the same irrespective of the amplitude of K_{11}. In the FFS mode using an LC with positive dielectric

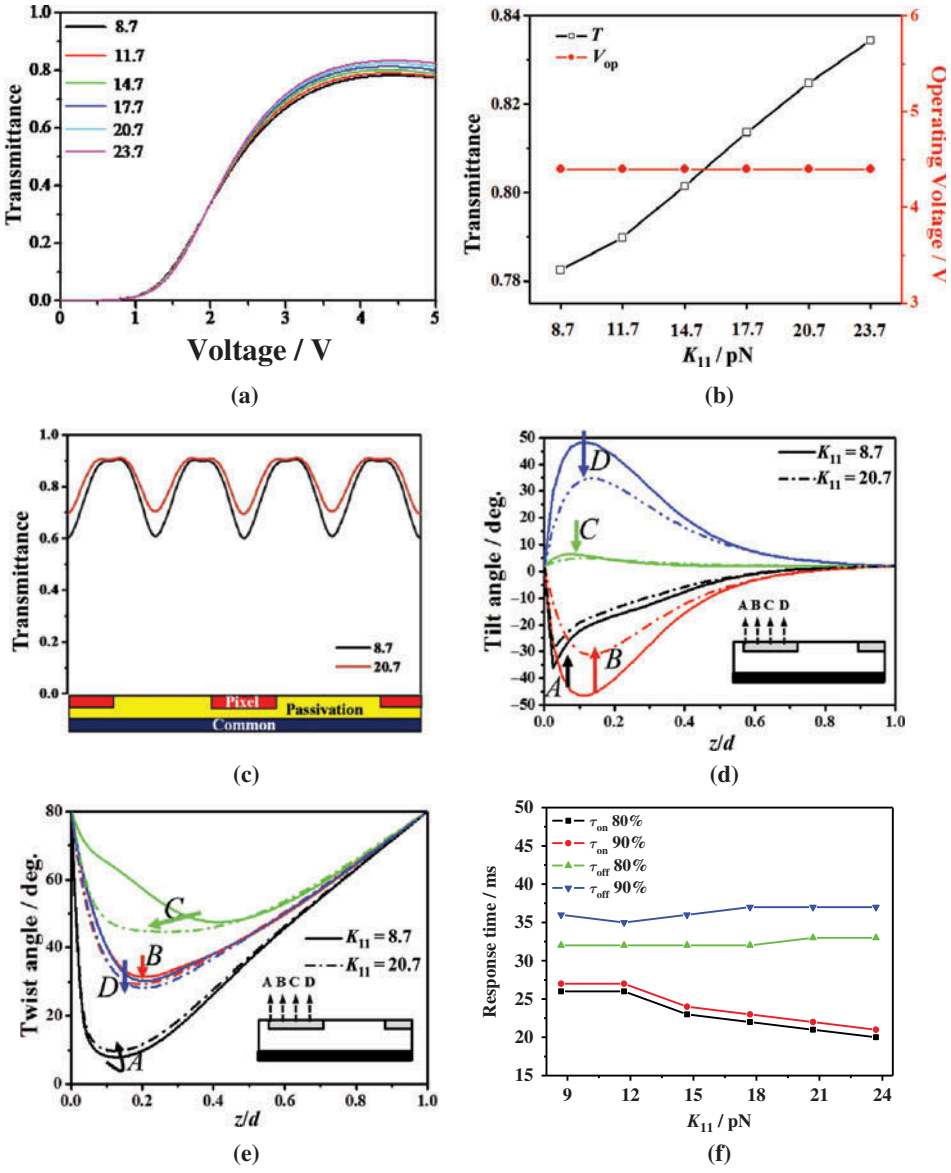

Figure 3. (colour online) (a) Voltage-dependent transmittance curves according to the variation of splay elastic constant (K_{11}); (b) summary of (a); (c) transmittance comparison along electrode position when K_{11} = 8.7 and 20.7 pN; (d) and (e) present the LC director profile in tilt and twist angles in four different electrode positions; and (f) presents response times according to the magnitude of splay elastic constant (K_{11}) at V_{op}. Here, the calculations are performed with K_{22} = 5.2 pN and K_{33} = 13.3 pN.

anisotropy, the homogeneously aligned LCs at an initial state reorient along the field direction with mainly twist deformation but also with tilt deformation as described in the switching principle. Therefore, K_{eff} cannot be simply replaced by K_{22} and must be associated with K_{22} and K_{11}. Nevertheless, the results clearly indicate that increasing K_{11} suppresses the tilt deformation of LC molecules (as already proved in the distribution of LC molecules according to two K_{11}s), which allows LCs to reorient with easier gliding when K_{11} becomes higher, resulting in a faster rise time although the applied voltages are the same for all cases. Nevertheless, suppressing a tilt deformation of LCs by increasing K_{11} does not affect τ_{off} much, which is purely associated with elastic energy difference between dark and white states.

3.2. *Electro-optic effects on twist elastic constant (K_{22})*

In IPS and FFS modes, K_{22} is very important because LC deformation is mainly associated with K_{22} so that V_{th} as well as response times of the device strongly depend on K_{22}. To investigate how electro-optic

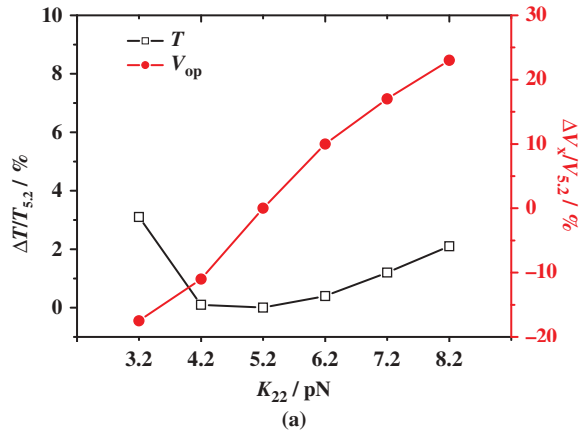

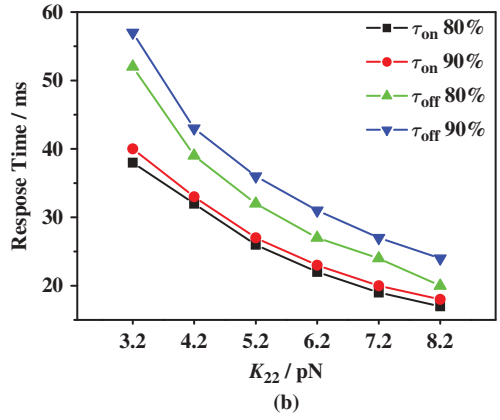

Figure 4. (colour online) (a) Change ratio in transmittance and operating voltage and (b) response times as a function of amplitude of twist elastic constants (K_{22}). Here, the calculations are performed with K_{11} = 8.7 pN and K_{33} = 13.3 pN and the number in subscript in transmittance and voltage change indicates the magnitude of K_{22}.

characteristics of the FFS device are affected by K_{22}, it was varied from 3.2 to 8.2 pN while keeping the rest of the parameters the same with K_{11} = 8.7 pN and K_{33} = 13.3 pN.

Figure 4(a) shows V–T curves in the FFS cell for different values of K_{22}, keeping other K values unchanged. In case of K_{22} = 3.2 pN, the V_{op} is 3.3 V and transmittance is 0.80. In case of K_{22} = 5.2 pN, the V_{op} is 4.0 V and the transmittance is 0.78. When K_{22} increases from 5.2 to 8.2 pN, the V_{op} becomes 4.9 V and the transmittance becomes 0.79. The increasing ratio of V_{op} with K_{22} simply follows the relationship of $V_{op} \propto \sqrt{K_{22}}$. Having low magnitude of K_{22} increases transmittance; however, the slight increase in transmittance with increasing K_{22} seems to be interesting because it is expected that the lower the K_{22}, the higher becomes the transmittance above the centres of pixel and common electrodes owing to easy twist deformation in a low K_{22}. The results imply that there might be an optimal ratio of K_{11}/K_{22} maximising transmittance.

Figure 4(b) shows calculated response times as a function of the amplitude of K_{22}s. As clearly indicated, the response times are proportional to $1/K_{22}$ such that the high magnitude of K_{22} in an LC mixture is favoured for achieving a fast response time although the V_{op} is increased with $\sqrt{K_{22}}$.

3.3. *Electro-optic effects on bend elastic constant (K_{33})*

Figure 5(a) presents the V–T curves according to the magnitude of K_{33} in the FFS cell. It is clear that there are no considerable changes in the V–T curves with changes in the magnitude of K_{33}, confirming that the influence on K_{33} is ignorable compared to K_{11} and K_{22} in case of transmittance. Figure 5(b) shows response times with the K_{33} value and it seems that the rise time and decay time slightly increases and decreases, respectively, with increasing K_{33}s within

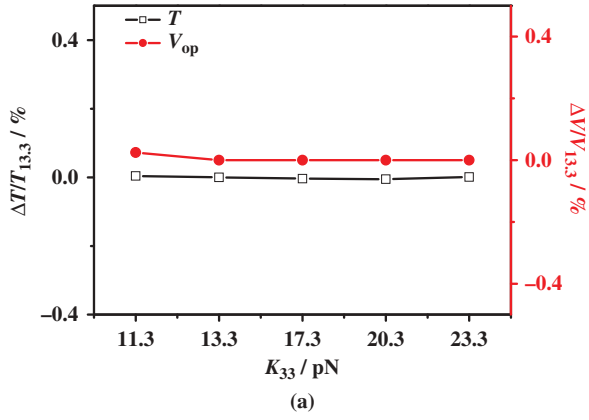

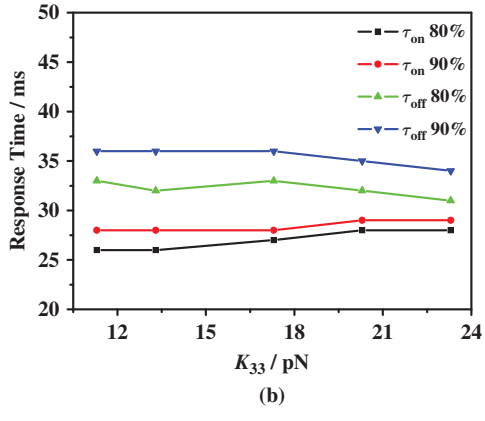

Figure 5. (colour online) (a) Transmittance and operating voltage and (b) response times as a function of amplitude of bend elastic constants (K_{33}). Here, the calculations are performed with K_{11} = 8.7 pN and K_{22} = 5.2 pN and the number in subscript in transmittance and voltage change indicates magnitude of K_{33}.

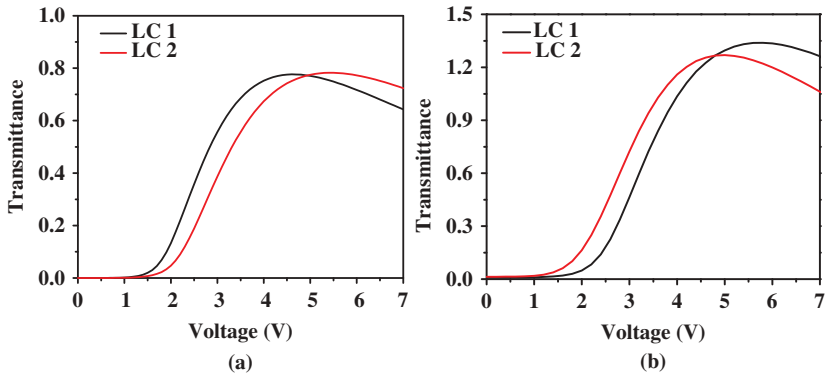

Figure 6. (colour online) Comparison of voltage-dependent transmittance curves between high and low elastic constant LCs with positive dielectric anisotropy: (a) simulation, (b) experiment.

few percentages, resulting in the total response time remaining about the same.

Summarising the effects of elastic constants on the electro-optic performances of the FFS mode for an LC with positive dielectric anisotropy based on the calculated results, interesting features appear such that (i) the higher K_{11} results in higher transmittance and faster rising time; however, the V_{op} is not affected; (ii) the higher K_{22} results in fast response time in a proportional relationship of $\tau \propto 1/K_{22}$ but the V_{op} increases for the relationship $V_{op} \propto \sqrt{K_{22}}$, at the same time, indicating that the V_{op} is mainly associated with K_{22} although deformations of K_{11} and K_{22} are involved during switching; (iii) the amplitude of K_{33} does not much affect the electro-optics of the FFS mode; (iv) the most effective ways to improve the transmittance and to have fast response times is to increase K_{11} and K_{22} of an LC, respectively.

3.4. Experimental confirmation of elastic constant effects on the FFS mode

In order to confirm theoretical results, we prepared two LC mixtures, LC1 and LC2, which have the same values of dielectric anisotropy ($\Delta\varepsilon$ = 5.1 at 1 kHz, 20°C) and birefringence (Δn = 0.1 at 589 nm, 20°C) but different elastic constants. The LC1 has K_{11} = 12.6 pN, K_{22} = 6.5 pN, K_{33} = 13.0 pN and the LC2 has K_{11} = 18.3 pN, K_{22} = 8.9 pN, K_{33} = 17.7 pN. The rotational viscosity γ of LC1 and LC2 at 20°C is 66 and 81 mPa s, respectively. Using two LCs, the FFS cells have been made with cell parameters such as signal electrode width w = 4.0 μm, a gap between signal electrodes l = 6.0 μm, respectively, and the passivation layer thickness = 0.29 μm, d = 3.8 μm, and the rubbing angle with respect to horizontal field component of a fringe electric field is 83°. Figure 6 shows V–T curves by simulation and experiment. Although the absolute values of a V_{op} are not the same each other between simulation and experimental results, the transmittance difference in LC1 and LC2 and the shape of the V–T curves show good agreements in simulation and experiments. The simulation results show that the FFS cell with LC2 shows better transmittance than that with LC1 by 1.4% (from 0.77 to 0.78) and the driving voltage is also increased by about 17.4% from 4.6 V (LC1) to 5.4 V (LC2). The experimental data exhibited the same trend as in the simulation, with an increase of 3.7% in transmittance, which is mainly associated with increase in K_{11} and about 16.0% increase in the driving voltage from 5.0 to 5.8 V, which is mainly associated with increase in K_{22} because the expected value using the relationship between V_{op} and K_{22} is 5.83 V (= $5.0 \times \sqrt{8.85/6.50}$). The difference in the increasing level between simulation and experimental results might be associated with measurement errors in cell and LC parameters. The response times are also measured for both LCs. The rise times are 18.3 and 15.9 ms, and the decay times are 15.7 and 14.6 ms for LC1 and LC2, respectively. Considering viscoelastic constant γ/K_{22} of LC1 and LC2, the ratios are about 10.15 and 9.10, respectively. If the response time is purely dependent on the viscoelastic constant, τ_{on} of LC2 should be about 16.4 ms (=18.3 ms × (9.10/10.15)), which is slightly higher value than the measured value of 15.9 ms. This also indicates that K_{11} needs to be taken into account in the viscoelastic constant such that K_{eff} should be replaced by ($K_{22} + \alpha K_{11}$), where α is an empirical constant. On the other hand, the τ_{off} seems to follow the magnitude of γ/K_{22} such that the expected value for LC2 is 14.1 ms (= 15.7 ms × (9.10/10.15)), which is slightly shorter than the measured value of 14.6 ms but in good agreement with the expected value.

4. Summary

The electro-optic characteristics of a FFS mode dependent on the elastic constants of a LC have been investigated. Especially with a positive dielectric anisotropic LC, tilt as well as twist deformation was experienced for the voltage-on state such that the magnitude of the two elastic constants K_{11} and K_{22} affects the electro-optic performance of the FFS mode. Results show that the higher the K_{11}, the higher the light efficiency, and the rise time becomes faster; and the higher the K_{22}, the faster the response time although the operating voltage becomes higher. The results are helpful to design LC mixtures in the FFS mode, which is widely used in all high-resolution and high image quality LCDs.

Disclosure statement

No potential conflict of interest was reported by the authors.

Funding

This research was supported by the National Research Foundation of Korea (NRF) Grant funded by the Korean Government (MSIP) [2014R1A4A1008140] and Polymer Materials Fusion Research Center.

References

[1] Lee SH, Lee SL, Kim HY. Electro-optic characteristics and switching principle of a nematic liquid crystal cell controlled by fringe-field switching. Appl Phys Lett. 1998;73:2881–2883. doi:10.1063/1.122617.

[2] Lee SH, Lee SL, Kim HY. High-transmittance, wide-viewing-angle nematic liquid crystal display controlled by fringe-field switching. Proc 18th Int Disp Res Conf. 1998:371–374.

[3] Lee SH, Lee SL, Kim HY, Eom TY. A novel wide-viewing-angle technology: ultra-trans view. SID Symp Dig Tech Pap. 1999;30:202–205. doi:10.1889/1.1833995.

[4] Lee SH, Lee SM, Kim HY, Kim JM, Hong SH, Jeong YH, Park CH, Choi YJ, Lee JY, Koh JW, Park HS. 18.1: Ultra-FFSTFT_LCD with super image quality and fast response time. SID Int Symp Dig Tech Pap. 2001;32:484–487. doi:10.1889/1.1831901.

[5] Noh JD, Kim HY, Kim JM, Koh JW, Lee JY, Park HS, Lee SH. Pixel structure of the Ultra-FFS TFT-LCD for strong pressure-resistant characteristic. J Soc Inf Disp. 2002;10:224–227. doi:10.1889/1.1830236.

[6] Lee SH, Bhattacharyya SS, Jin HS, Jeong KU. Devices and materials for high-performance mobile liquid crystal displays. J Mater Chem. 2012;22:11893–11903. doi:10.1039/C2JM30635B.

[7] Kim DH, Lim YJ, Kim DE, Ren H, Ahn SH, Lee SH. Past, present, and future of fringe-field switching-liquid crystal display. J Inf Disp. 2014;15:99–106. doi:10.1080/15980316.2014.914982.

[8] Lee SH, Lee SL, Kim HY, Eom TY. Analysis of light efficiency in homogeneously aligned nematic liquid crystal display with interdigital electrodes. J Kor Phys Soc. 1999;35:S1111–S1114. doi:10.3938/jkps.35.1111.

[9] Yun HJ, Jo MH, Jang IW, Lee SH, Ahn SH, Hur HJ. Achieving high light efficiency and fast response time in fringe field switching mode using a liquid crystal with negative dielectric anisotropy. Liq Cryst. 2012;39:1141–1148. doi:10.1080/02678292.2012.700078.

[10] Jo MH, Yun HJ, Jang IW, Jeong IH, Lee SH, Cho SH, Ahn SH, Heo HJ. Electro-optic characteristics of the fringe in-plane switching liquid crystal device for a liquid crystal with negative dielectric anisotropy. Liq Cryst. 2013;40:368–373. doi:10.1080/02678292.2012.749307.

[11] Yu IH, Song IS, Lee JY, Lee SH. Intensifying the density of a horizontal electric field to improve light efficiency in a fringe-field switching liquid crystal display. J Phys D Appl Phys. 2006;39:2367–2372. doi:10.1088/0022-3727/39/11/009.

[12] Park JW, Ahn YJ, Jung JH, Lee SH, Lu R, Kim HY, Wu ST. Liquid crystal display using combined fringe and in-plane electric fields. Appl Phys Lett. 2008;93:081103. doi:10.1063/1.2973152.

[13] Jo MH, Yun HJ, Jang IW, Jeong IH, Lee SH, Cho SH, Ahn SH, Heo HJ. Electro-optic characteristics of the fringe in-plane switching liquid crystal device for a liquid crystal with negative dielectric anisotropy. Liq Cryst. 2013;40:368–373. doi:10.1080/02678292.2012.749307.

[14] Hong SH, Park IC, Kim HY, Lee SH. Electro-optic characteristic of fringe-field switching mode depending on rubbing direction. Jpn J Appl Phys. 2000;39:L527–530. doi:10.1143/JJAP.39.L527.

[15] Jung SH, Kim HY, Song SH, Kim JH, Nam SH, Lee SH. Analysis of optimal phase retardation of a fringe field-driven homogeneously aligned nematic liquid crystal cell. Jpn J Appl Phys. 2004;43:1028–1031. doi:10.1143/JJAP.43.1028.

[16] Kim SJ, Song IS, Lee SH, Kim HY, Kim SY, Lim YJ. Optimal cell retardation value of a fringe-field switching mode using a liquid crystal with negative dielectric anisotropy. Mol Cryst Liq Cryst. 2006;449:87–94. doi:10.1080/15421400600582507.

[17] Jung SH, Kim HY, Lee MH, Rhee JM, Lee SH. Cell gap-dependent transmission characteristics of a fringe-electric field driven homogeneously aligned liquid crystal cell, for a liquid crystal with negative dielectric anisotropy. Liq Cryst. 2005;32:267–275. doi:10.1080/02678290412331329233.

[18] Kim SJ, Kim HY, Lee SH, Lee YK, Park KC, Jang J. Cell gap-dependent transmittance characteristic in a fringe field-driven homogeneously aligned liquid crystal cell with positive dielectric anisotropy. Jpn J Appl Phys. 2005;44:6581–6586. doi:10.1143/JJAP.44.6581.

[19] Kim HY, Nam SH, Lee SH. Dynamic stability of the fringe-field switching liquid crystal cell depending on dielectric anisotropy of a liquid crystal. Jpn J Appl Phys. 2003;42:2752–2755. doi:10.1143/JJAP.42.2752.

[20] Ryu JW, Lee JY, Kim HY, Park JW, Lee GD, Lee SH. Effect of magnitude of dielectric anisotropy of a liquid crystal on light efficiency in the fringe-field switching nematic liquid crystal cell. Liq Cryst. 2008;35:407–411. doi:10.1080/02678290801919659.

[21] Jung JH, Ha KS, Srivastava AK, Lee HK, Lee SE, Lee SH. Light efficiency of the fringe-field switching mode depending on magnitude of dielectric anisotropy of liquid crystal associated with cell gap and rubbing angle. J Kor Phys Soc. 2010;56:548–553. doi:10.3938/jkps.56.548.

[22] Kang SW, Jang IW, Kim DH, Lim YJ, Lee SH. Enhancing transmittance of fringe-field switching liquid crystal device by controlling perpendicular component of dielectric constant of liquid crystal. Jpn J Appl Phys. 2014;53:010304. doi:10.7567/JJAP.53.010304.

[23] Oh EM, Kondo K. Electro-optical characteristics and switching behavior of the in-plane switching mode. Appl Phys Lett. 1995;67:3895–3897. doi:10.1063/1.115309.

[24] Lien A. Extended Jones matrix representation for the twisted nematic liquid-crystal display at oblique incidence. Appl Phys Lett. 1990;57:2767–2769. doi:10.1063/1.103781.

[25] Lim YJ, Choi YE, Lee JH, Lee GD, Komitov L, Lee SH. Effects of three-dimensional polymer networks in vertical alignment liquid crystal display controlled by in-plane field. Opt Express. 2014;22:10634. doi:10.1364/OE.22.010634.

[26] Yang DK, Wu ST. Fundamentals of liquid crystal devices. Chichester: John Wiley & Sons; 2006. ISBN: 978-0-470-01542-1.